/
Article / Book Information

Title	Static and dynamic characteristics of double transverse coupled cavity VCSELs for high speed modulations
	Hameeda Ragab Ibrahim, AHMED MAGDI MUSA, ,
Authors	Hameeda R Ibrahim, Ahmed MA Hassan, Xiaodong Gu, Moustafa Ahmed, Fumio Koyama
	, Vol. 18, No. 22, p. 20210419
Citation	IEICE Electronics Express, Vol. 18, No. 22, p. 20210419
/Pub. date	2021, 11
/Copyright	Copyright(c) 2021 IEICE

Static and dynamic characteristics of double transverse coupled cavity VCSELs for high speed modulations

Hameeda R Ibrahim[1, 2, a)], **Ahmed MA Hassan**[1, 3], **Xiaodong Gu**[1, 4], **Moustafa Ahmed**[2, 5], and **Fumio Koyama**[1]

Abstract   We present experimental results for extending the 3-dB modulation bandwidth of an 850-nm vertical-cavity surface-emitting laser (VCSEL) with passive double transverse-coupled cavities (DTCC). The 3-dB modulation bandwidth of DTCC-VCSEL is 21 GHz while that of a conventional VCSEL (C-VCSEL) fabricated in the same wafer is 12 GHz. We realize eye-opening at large-signal modulations of 36 Gbps (NRZ) and 44 Gbps (PAM4). Intensity fluctuations of single-transverse-coupled cavity (STCC)-VCSEL and DTCC-VCSEL were also examined at different bias currents under CW operations. The result shows a DTCC-VCSEL is more stable with lower intensity fluctuations.
Keywords: VCSEL, TCC-VCSEL, DTCC-VCSEL, OFB
Classification: Semiconductor lasers

1.   Introduction

A VCSEL has played a major role for optical data transmissions in datacenters and supercomputers because of its attractive properties [1, 2], which include low power consumption, small footprint, wafer-scale testing, low-cost packaging, ease of fabrication into arrays, and so on. The modulation bandwidth of VCSELs, however, is typically restricted to less than ~20 GHz because of the limited intrinsic carrier-photon resonance (CPR) [3]. Therefore, intensive efforts have been done to push the modulation bandwidth of VCSELs further into the mm-wave band [4, 5, 6, 7, 8, 9, 10, 11, 12, 13, 14, 15, 16, 17] such as injection-locking [18, 19], coupled cavity [20], modulator-integration [21] and optical feedback (OFB) [22, 23, 24, 25, 26, 27]. OFB has been used for increasing the modulation bandwidth of VCSELs [22], mode stabilization, and the reduction of modulation-induced frequency chirp [28]. We also proposed a double transverse-coupled cavities (DTCC)-VCSEL for further increase in modulation

bandwidths [29], which predicted ultra-high speed modulation of > 100 Gbps [30].

In this paper, we fabricated a DTCC-VCSEL with a taper shaped aperture. We demonstrate the enhancement of modulation bandwidth of DTCC-VCSELs. The 3-dB modulation bandwidth could be increase more than 20 GHz and we realized eye-opening at the large-signal modulation of 36 Gbps (Non-Return-to-Zero:NRZ) and 44 Gbps (Pulse Amplitude Modulation 4-level:PAM4).

2.   Device structure

Figure 1 illustrates the schematic structure of a DTCC-VCSEL and the top view of fabricated mesas for C-VCSEL, STCC and DTCC-VCSELs.   All devices including C-VCSELs are fabricated on a same wafer grown by metal organic chemical vapor deposition (MOCVD) with 22-pair top DBR and 34-pair bottom DBR. The active region includes three 850 nm quantum wells (3QWs).   In order to form transverse coupled cavity structures, taper shaped mesas were formed by dry-etching process and followed by wet-oxidation process. The active region dimensions of a DTCC-VCSEL are $6 \times 5\,\mu m^2$, the oxidation depth is $5\,\mu m$. The size of passive cavities for DTCC-VCSEL is $30 \times 13\,\mu m^2$ and $15 \times 13\,\mu m^2$ respectively. The proton ion implantation is carried out for electric isolations in coupled cavities. The width and total depth of the multi-step implantation is $2\,\mu m$ and $2.8\,\mu m$, respectively. Polyamide is used for planarization and passivation. For making a surface N-electrode, wet etching is used, and AuGe/Ni/Au are deposited to form the N-electrode. For P-electrode Au/Zn/Au are deposited.
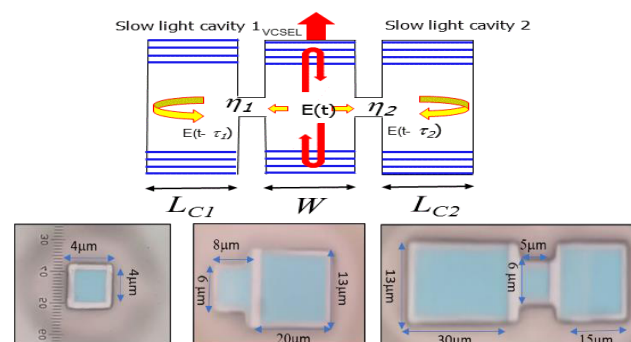

Fig. 1   (a) Schematic structure of a DTCC-VCSEL, (b) photos of fabricated mesas for C-VCSEL, STCC and DTCC-VCSELs.

[1] Institute of Innovative Research, Tokyo Institute of Technology, 4259-R2-22, Nagatsuta-cho, Midori-ku, Yokohama, 226-8503 Japan

[2] Department of Physics, Faculty of Science, Minia University, 61519 Minia, Egypt

[3] Department of Physics, Faculty of Science, Al-Azhar University, Assuit, Egypt

[4] Ambition Photonics Inc., Tokyo Tech Yokohama Venture Plaza E208, Yokohama, 226-8510 Japan

[5] Department of Physics, Faculty of Science, King Abdulaziz University, 80203 Jeddah21589, Saudi Arabia

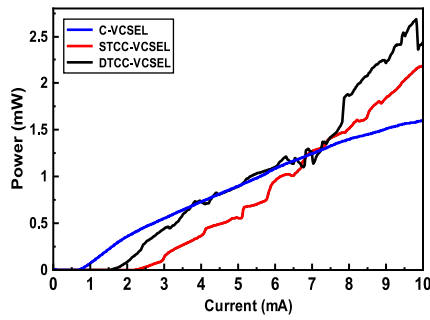a) ibrahim.h.aa@m.titech.ac.jp

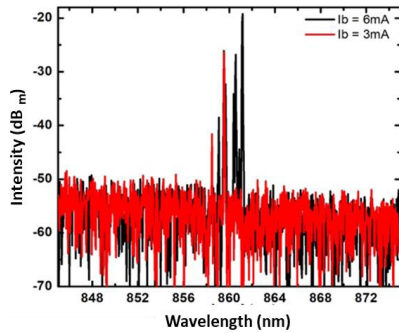**Fig. 2** L-I characteristics for C-VCSEL, STCC VCSEL and DTCC-VCSEL.

**Fig. 3** Lasing spectra of DTCC-VCSEL.

3. Results and discussions

Figure 2 show I-L characteristics of a conventional VC-SEL (C-VCSEL), STCC and DTCC-VCSELs fabricated on the same wafer at room temperature for comparison. The threshold current of the DTCC-VCSEL is 1.8 mA that is higher than that of the C-VCSEL due to an optical loss in the implanted region and to the leakage in two external cavities. The active region area of a C-VCSEL, STCC-VCSEL and DTCC-VCSEL are $4 \times 4\,\mu m^2$, $6 \times 8\,\mu m^2$ and $6 \times 5\,\mu m^2$, respectively. The size of passive cavity for STCC-VCSEL is $20 \times 13\,\mu m^2$. The size of passive cavities for DTCC-VCSEL is $30 \times 13\,\mu m^2$ and $15 \times 13\,\mu m^2$. The L-I curve of C-VCSEL is smooth and the power increases linearly with injection current. L-I curves for STCC and DTCC-VCSELs show many kinks due to the effect of OFB. Figure 3 shows the lasing spectra of the DTCC-VCSEL at different bias currents.

Figure 4(a) shows the small signal response of a C-VCSEL at room temperature. The 3-dB bandwidth without optical feedback is around 9 GHz at 3.5 mA increases to 12 GHz at 6 mA. But the 3-dB bandwidth drops by increasing the bias current due to a heating effect.

The small-signal modulation response of a STCC-VCSEL with $6 \times 8\,\mu m^2$ active region and the size of a passive cavity are $25 \times 23\,\mu m^2$ at different bias currents are shown in Fig. 4(b) The modulation bandwidth of VCSEL is 16.7 GHz at 4 mA, by increasing the bias current to 4.5 mA, the modulation bandwidth increased to 27 GHz thanks to PPR which appears clearly at 25 GHz because of optical feedback. When the bias current increases to 4.7 and 5.0 mA the modulation response decreases to 12.3 GHz and 11.3 GHz respectively. The rapid drop of the modulation bandwidth
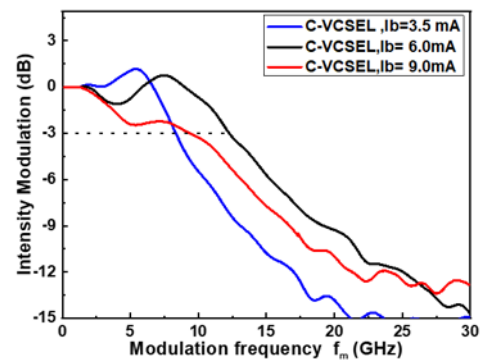
(a)
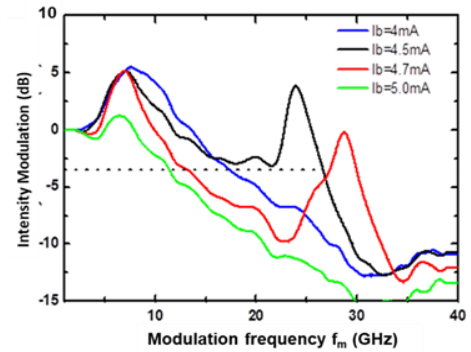
(b)
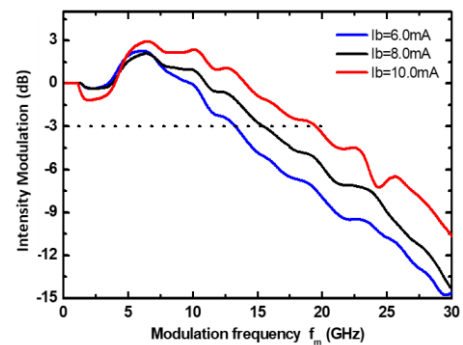
(c)

Fig. 4 Small signal responses of (a) C-VCSEL, (b) STCC-VCSEL and (c) DTCC-VCSEL with different injection currents.

would be due to the heating effect, which deteriorates the coupling between the active main cavity and passive cavity.

The small-signal modulation response of DTCC-VCSEL is shown in Fig. 4(c) at different bias currents. The modulation bandwidth of DTCC-VCSEL is 13 GHz at 6 mA. With increasing the bias current to 8 mA and 10 mA the modulation bandwidth increased to 16 GHz and 21 GHz due to OFB without drop in modulation response because the large area of DTCC-VCSEL and thermal spread which decrease the heat effect comparing with the STCC-VCSEL.

Low intensity fluctuations are important for large signal modulations. The TCC-VCSEL dynamics strongly depend on the bias current and optical feedback parameters. We found the intensity fluctuations of a STCC-VCSEL are dependent on the bias current, which could result from the instability of a VCSEL under OFB. We discussed the intensity fluctuation of coupled cavity VCSELs in ref. [31], which is dependent on the bias current and coupling strength. These
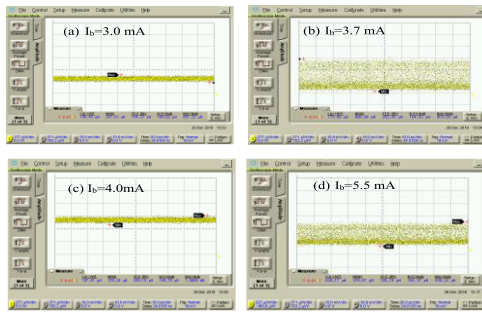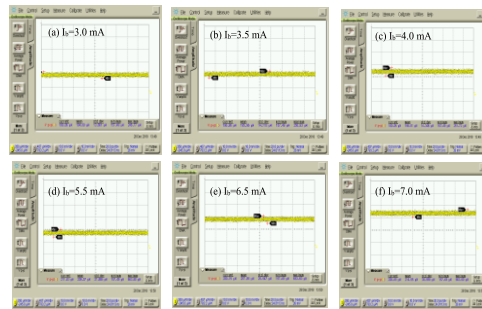
Fig. 5 Intensity fluctuations of a STCC-VCSEL.

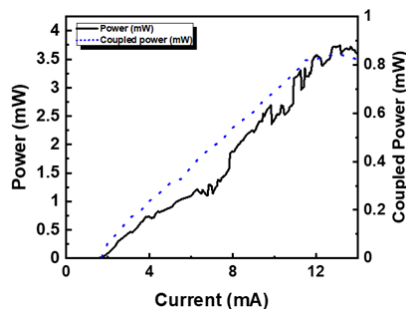**Fig. 6** Intensity fluctuations of a DTCC-VCSEL.

Fig. 7 Coupling strength of DTCC-VCSEL.

also could affect the appearance of PPR shown in Fig. 4(b). We could see the large intensity fluctuation at a certain bias current, which makes it difficult to get clear eye opening of large signal modulations. In contrast, the intensity fluctuations of DTCC-VCSEL are shown in Fig. 6(a)–(b), the intensity fluctuations are suppressed in the entire current range due to different coupling strengths of around 25% as shown as Fig. 7, which is supported by the calculation [31].

We carried out the large signal modulations with NRZ and PAM4. The large signal modulation characteristics are shown in Figs. 8 show the eye patterns (NRZ) for C-VCSEL, STCC-VCSEL and DTCC-VCSEL at room temperature. The bias current is 9 mA and an extinction ratio is 3.5 dB. The word length is $2^{31} - 1$. The clear eye-opening was observed for a DTCC-VCSEL at 36 Gbps. The bandwidth of the C-VCSEL is limited for 20 Gbps. While the small signal modulation bandwidth is higher, it is hard to get clear eye-opening, which is due to the increased intensity fluctuations in STCC-VCSELs. Figures 9 shows large signal modulations (PAM-4) of C-VCSEL and DTCC-VCSEL at B=20 and 22 Gbaud with I_b=10 mA. The modulation bandwidth enhancement comes from OFB. Wider bias current
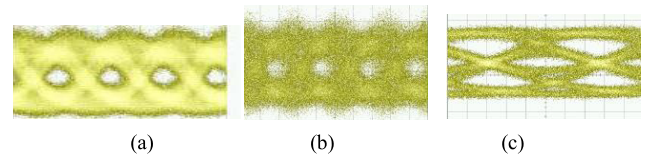

Fig. 8 Large signal modulations (NRZ) of (a) C-VCSEL at 20 Gbps, (b) STCC-VCSEL at 40 Gbps and (c) DTCC-VCSEL at 36 Gbps.
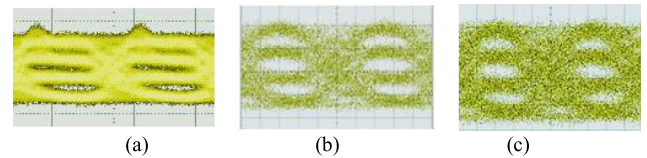

Fig. 9 Large signal modulations (PAM4) of (a) C-VCSEL at 10 Gbaud DTCC-VCSEL at (b) 20 Gbaud and (c) 22 Gbaud.

ranges could be possible for lower intensity fluctuations and high modulation bandwidths of DTCC-VCSELs in contrast to STCC-VCSELs. While higher modulation bandwidths of coupled cavity VCSELs have been reported by other research groups [27, 32], there have been no report of large signal modulations. Intensity fluctuations should be an important issue for practical applications.

4. Conclusion

The transfer function of IM response in VCSELs can be tailored by double transverse coupled cavities, which exhibit a large enhancement in the modulation bandwidth. While a STCC-VCSEL shows a high modulation bandwidth of 27 GHz, it is noted that the bias current window is rather limited for low intensity fluctuations and high modulation bandwidths. The 3-dB modulation bandwidth of DTCC-VCSELs reaches at 21 GHz and a clear eye-pattern of 36 Gbps (NRZ) and 44 Gbps (PAM-4) operation was also obtained. Wider bias current ranges could be possible for lower intensity fluctuations and high modulation bandwidths in contrast to STCC-VCSELs.

Acknowledgments

References

[1] K. Iga: "Vertical-cavity surface-emitting laser: Its conception and evolution," Jpn. J. Appl. Phys. **47** (2008) 1 (DOI: 10.1143/JJAP.47.1).

[2] F. Koyama: "Recent advances of VCSEL photonics," J. Lightw. Technol. **24** (2006) 4502 (DOI: 10.1109/JLT.2006.886064).

[3] N. Suzuki, et al.: "High speed 1.1-µm-range InGaAs-based VC-SELs," IEICE Trans. Electron. **E92-C** (2009) 942 (DOI: 10.1587/transele.E92.C.942).

[4] A. Larsson, et al.: "High speed VCSELs and VCSEL arrays for single and multicore fiber lnterconnects," Proc. SPIE **9381** (2015) 93810D-1 (DOI: 10.1117/12.2082614).

[5] D.M. Kuchta, et al.: "A 71-Gb/s NRZ modulated 850-nm VCSEL-based optical link," IEEE Photon. Technol, Lett. **27** (2015) 577 (DOI: 10.1109/LPT.2014.2385671).

[6] W.H.S. Wanckel and H.E. Hofmann: "Small-signal analysis of ultra-high-speed multi-mode VCSELs," IEEE J. Quantum Electron. **52**

(2016) 2400311 (DOI: 10.1109/JQE.2016.2574540).

[7] D.M. Kuchta, *et al*.: "A 56.1 Gb/s NRZ modulated 850 nm VCSEL-based optical link," OSA/OFC (2013). (DOI: 10.1364/OFC.2013.OW1B.5).

[8] W. Hamad, *et al*.: "Small-signal analysis of high-performance VCSELs," IEEE Photon. J. **11** (2019) 1501212 (DOI: 10.1109/JPHOT.2019.2901722).

[9] P. Westbergh, *et al*.: "High-speed 850 nm VCSELs operating error free up to 57 Gbit/s," Electron. Lett. **49** (2013) 1021 (DOI: 10.1049/el.2013.2042).

[10] P. Bardella and I. Montrosset: "A new design procedure for DBR lasers exploiting the photon–photon resonance to achieve extended modulation bandwidth," IEEE J. Sel. Topics Quantum Electron. **19** (2013) 1502408 (DOI: 10.1109/JSTQE.2013.2250260).

[11] K. Szczerba, *et al*.: "60 Gbits error-free 4-PAM operation with 850 nm VCSEL," Electron. Lett. **49** (2013) 953 (DOI: 10.1049/el.2013.1755).

[12] S.T.M. Fryslie, *et al*.: "37-GHz modulation via resonance tuning in single-mode coherent vertical-cavity laser arrays," IEEE Photon. Technol, Lett. **27** (2015) 415 (DOI: 10.1109/LPT.2014.2376959)

[13] C.H. Cheng, *et al*.: "850/940-nm VCSEL for optical communication and 3D sensing," Opto-Elect. Adv. **1** (2018) 180005 (DOI: 10.29026/oea.2018.180005).

[14] D. Kuchta, *et al*.: "64 Gb/s transmission over 57 m MMF using an NRZ modulated 850 nm VCSEL," Proc. Opt. Fiber Commun. Conf. (2014) Th3C.2 (DOI: 10.1364/OFC.2014.Th3C.2).

[15] E. Haglund, *et al*.: "30 GHz bandwidth 850 nm VCSEL with sub-100 fJ/bit energy dissipation at 25–50 Gbit/s," Electron. Lett. **51** (2015) 1096 (DOI: 10.1049/el.2015.0785).

[16] E. Haglund, *et al*.: "High-speed VCSELs with strong confinement of optical fields and carriers," J. Lightw. Technol. **34** (2016) 269 (DOI: 10.1109/JLT.2015.2458935).

[17] M. Liu, *et al*.: "50 Gb/s error-free data transmission of 850 nm oxide-confined VCSELs," Proc. OFC (2016) Tu3D.2 (DOI: 10.1364/OFC.2016.Tu3D.2).

[18] X. Zhao, *et al*.: "Novel cascaded injection-locked 1.55-µm VCSELs with 66 GHz modulation bandwidth," Opt. Exp. **15** (2007) 14810 (DOI: 10.1364/OE.15.014810).

[19] S.H. Lee, *et al*.: "Bandwidth enhancement of injection-locked distributed reflector lasers with wire like active regions," Opt. Exp. **18** (2010) 16370 (DOI: 10.1364/OE.18.016370).

[20] C. Chen and K.D. Choquette: "Analog and digital functionalities of composite-resonator vertical-cavity lasers," J. Lightw. Technol. **28** (2010) 1003 (DOI: 10.1109/JLT.2010.2041747).

[21] A. Paraskevopoulos, *et al*.: "Ultra-high-bandwidth (> 35 GHz) electrooptically-modulated VCSEL," OFC/NFOES 2006 (2006) PDP22 (DOI: 10.1109/OFC.2006.216055).

[22] H. Dalir and F. Koyamad: "Bandwidth enhancement of single-mode VCSEL with lateral optical feedback of slow light," IEICE Electron. Exp. **8** (2011) 1075 (DOI: 10.1587/elex.8.1075).

[23] H. Dalir and F. Koyama, "29 GHz directly modulated 980 nm vertical-cavity surface emitting lasers with bow-tie shape transverse coupled cavity," Appl. Phys. Lett. **103** (2013) 091109 (DOI: 10.1063/1.4820149).

[24] H. Dalir and F. Koyama: "High-speed operation of bow-tie-shaped oxide aperture VCSELs with photon–photon resonance," Appl. Phys. Express **7** (2014) 022102 (DOI: 10.7567/APEX.7.022102).

[25] M. Ahmed, *et al*.: "Enhancing the modulation bandwidth of VCSELs to the millimeter-waveband using strong transverse slow-light feedback," Optics Express **23** (2015) 15365 (DOI: 10.1364/OE.23.015365).

[26] X. Gu, *et al*.: "850 nm transverse-coupled-cavity vertical-cavity surface-emitting laser with direct modulation bandwidth of over 30 GHz," Appl. Phys. Express **8** (2015) 082702 (DOI: 10.7567/APEX.8.082702).

[27] S.T.M. Fryslie, *et al*.: "37-GHz modulation via resonance tuning in single-mode coherent vertical-cavity laser arrays," IEEE Photon. Technol. Lett. **27** (2015) 415 (DOI: 10.1109/LPT.2014.2376959).

[28] S. Hu, *et al*.: "Low chirp and high-speed operation of transverse coupled cavity VCSEL," Japanese Journal of Applied Physics **54** (2015) 090304 (DOI: 10.7567/JJAP.54.090304).

[29] H. Ibrahim, *et al*.: "Modulation bandwidth enhancement of double transverse coupled cavity VCSELs," 21st Microoptics Conference, (2016) 13A-7.

[30] H. Ibrahim, *et al*.: "Design of 100 Gbps double transverse coupled cavity VCSELs," 22nd Microoptics Conference (2017) (DOI: 10.23919/MOC.2017.8244494).

[31] H. Ibrahim, *et al*.: "Modelling and characterization of the noise characteristics of the vertical cavity surface-emitting lasers subject to slow light feedback," Pramana **93** (2019) 72 (DOI: 10.1007/s12043-019-1831-2).

[32] E. Heidari, *et al*.: "Hexagonal transverse-coupled-cavity VCSEL redefining the high-speed lasers," Nanophotonics **9** (2020) 743 (DOI: 10.1515/nanoph-2020-0437).